

RESEARCH ARTICLE



High Step Up Converter with Transformerless Inverter for Grid Integration

 OPEN ACCESS

Received: 18-06-2021

Accepted: 31-05-2022

Published: 30-08-2022

Y Sukhi^{1*}, Y Jeyashree², S Anita¹, A Jenifer¹, A Fayaz Ahamed¹¹ EEE Department, R.M.K. Engineering College, Thiruvallur, Tamilnadu, 601206, India² EEE Department, SRM University, Kattamkulathur, Tamilnadu, 603203, India

Citation: Sukhi Y, Jeyashree Y, Anita S, Jenifer A, Ahamed AF (2022) High Step Up Converter with Transformerless Inverter for Grid Integration. Indian Journal of Science and Technology 15(34): 1655-1665. <https://doi.org/10.17485/IJST/V15I34.1131>

* Corresponding author.

ysi.eee@rmkec.ac.in**Funding:** None**Competing Interests:** None

Copyright: © 2022 Sukhi et al. This is an open access article distributed under the terms of the [Creative Commons Attribution License](https://creativecommons.org/licenses/by/4.0/), which permits unrestricted use, distribution, and reproduction in any medium, provided the original author and source are credited.

Published By Indian Society for Education and Environment ([iSee](https://www.isee.org/))

ISSN

Print: 0974-6846

Electronic: 0974-5645

Abstract

Objectives: The objective of this paper is to design a high step up converter for PV applications. The output of the converter is applied to an inverter with less number of component counts. **Methods:** Coupled inductor is proposed in power electronic converters to increase high gain. The output of the dc-dc converter is given to the inverter. **Finding:** Simulation and hardware results show that the voltage stress in the passive components and the switches is reduced. Highly stable output voltage is obtained in the output due to high step up conversion. The converter can be operated in high step up mode without reaching the extreme limits. The leakage occurring in the coupled inductor is utilized and the problem due to reverse recovery voltage across the diode is reduced. Since low voltage is applied to MOSFET, conduction losses are less with higher efficiency. The inverter has a simple structure and operates at grid frequency. The inverter developed has low THD, better output waveform and the filter elements are of small size. The electromagnetic interference of the proposed inverter is very less. **Novelty:** The proposed inverter is designed with less number of switches. The proposed topology is simulated and the hardware is developed to know the feasibility of the converter.

Keywords: photovoltaic cell; harmonics; high step up converter; multilevel inverter; transformerless

1 Introduction

A Photovoltaic (PV) system uses a high step up converter for energy conversion^(1,2). Power electronic converters are widely used in the power conversion process of the PV system with a boost converter used with high duty ratio^(3,4). The voltage gain is limited by the passive elements used and the switches in the circuit. The use of a high duty ratio results in reverse recovery problems. There are many topologies designed to operate without the use of a high duty ratio. DC-DC converter in flyback configuration provides high step up gain with a simple structure. This converter uses electrical isolation and the switches in the circuit are subjected to more stress due to the leakage inductance^(5,6). There are energy regeneration techniques implemented to recycle the leakage energy. But a coupled inductor is utilized in the dc-dc converter to

provide high gain with low losses and low stress in the switching devices. Also, these converters make use of low duty ratio for high gain. When the system is developed to supply ac loads, the dc-ac converter can be in parallel with the solar panel. A Step up transformer or a series connection of solar panels can increase the voltage level required for the inverter^(7,8). Transformerless dc-dc converters like cascade boost type, voltage multiplier type, voltage lift type etc., achieve high gain are complex in structure and are not economical^(9,10). Eventhough the modified boost type is simple in structure, it uses three switches in the on state and two switches during off state. Grid connected PV systems are more demandable than off grid systems. PV systems with transformers are more costly and are complex as compared with transformerless PV systems. A PV system has common mode current, if the PV panel is not grounded. If the PV panel is not grounded, PV current in the low voltage side will have more ripples^(11,12). Since maximum power extraction from solar panels is difficult, algorithms are used in the conversion process. In between the PV panel and the inverter, the DC-DC converter changes low voltage from the PV panel to high voltage, required for the inverter. In the DC-DC converter maximum power point tracking is employed to utilize the solar energy to the maximum extent. In the maximum power tracking, steady state response is important⁽¹³⁾. When more than one converter is connected in series, the overall efficiency of the converter depends upon the efficiency of each converter. This leads to optimization of efficiency of each converter. The efficiency of the converter is increased using a single converter in this paper. There are different MPPT algorithms developed to achieve high accuracy and stable operations. P & O algorithm is used to get the maximum power tracking. Transformerless grid connected PV system is taken into consideration due to its advantages like better efficiency, smaller size and economical to some extent. The absence of an isolating transformer makes the system free from leakage problems, stray power losses and degraded quality of current. There is a great challenge in increasing the PV panel output voltage directly without the use of a step up converter. In this case, PV panels in series increase the voltage level to the grid voltage. Inverters with buck operation require increased power processing. This may result in high losses. Using multilevel inverters, it is possible to reduce the harmonic content in the output voltage for medium as well as high voltage loads. In the PV applications, a dc-dc converter is used in the front end before the dc-ac conversion at the back end. The different types of multilevel inverter are connected to the dc-dc converter either directly or indirectly. Diode clamped inverter uses a number of diodes and also creates unbalance in the system parameters. Similarly, a flying capacitor type inverter uses more capacitors which occupies more space. The development of the paper is done as below. The proposed structure principle of operation is discussed in section II. The DC-DC converter used for the voltage level conversion is discussed in section III. The MPPT algorithm used for the maximum power transfer is discussed in section IV. The inverter used in the proposed topology is discussed in section V. The mathematical analysis is discussed in section VI. The simulation of the developed system and experimental results taken using the prototype are discussed in section VII. The discussion based on the results obtained for the developed structure is done in section VIII. Conclusion of the proposed structure is discussed in section IX.

2 Principle of Operation

In the proposed system for PV energy conversion, a coupled inductor is used to provide high step up voltage conversion. The high step-up converter consists of a high voltage circuit, medium voltage circuit, clamped circuit and low voltage side circuit. The elements used in the first string are explained as follows. The low voltage side circuit consists of PV₁, capacitor C₁, primary inductor L_{P1} and the main switch Q₁. The clamped circuit is formed by the elements C_{L1} and D_{LI}. The middle voltage circuit is constituted by the inductor N_{S1}, capacitor C_{H1} and the diode D_{C1}. The elements in the high voltage side are D_{H1} and V_{S1}. The input voltage and current in the low voltage side are represented as v_{in1}, v_{in2}, i_{in1} and i_{in2}. In the high step up converter stage, the capacitors C₁ and C₂ represents the filter capacitor in the low voltage side, C_{S1} and C_{S2} represent the filter capacitor in the high voltage side, C_{L1} and C_{L2} are the clamped circuit capacitors, C_{H1} and C_{H2} are the middle voltage storage capacitors. The conventional multilevel inverter has power stages and a complex control circuit. Figure 1 shows the circuit diagram uses transformer-less five-level inverter topology. The conventional cascaded H bridge (CCHB) five level inverters use eight power switches. This proposed topology has only six power switches. In addition to this, the complexity of the power circuit reduces. This provides a simple design of the modulator circuit and its implementation. The phase shift control of PWM pulses is used to produce switching pulses. There are five different voltage levels produced in the output which are named as 2V_S, V_S, 0, -V_S, and -2V_S. PWM signals are generated for the inverter using carrier signal and reference signal. Here comparators are used for the generation of identical carrier signals. High frequency switching signals required for the switches S_{A1}, S_{B1}, S_{A3}, and S_{B3} operation are generated using carrier signals. Another comparator is used for zero-crossing detection to provide line-frequency switching signals for switches S_{A2} and S_{B2}. In this circuit, two voltage sources are used with the input potential V_{S1} and V_{S2}. In order to achieve the positive voltage, the switches S_{A1}, S_{A2} and S_{B3} will conduct. The current starts from the positive of voltage source V_{S2} and flows through the switch S_{A1}, S_{A2}, resistance, switch S_{B3} and ends with the negative of voltage source V_{S2}. To achieve the positive peak voltage the switches S_{A1}, S_{B1} and S_{B3} will conduct. The current starts from voltage source V_{S1} and flows through the switch S_{b1} and through resistance and switch S_{b3} and with the voltage source V_{S2} and S_{A2} and ends with voltage

source V_{S1} . To achieve the zero voltage, the switches S_{A1} , S_{A2} and S_{A3} will conduct. The current starts from the voltage source and flows through the switch S_{A1} and through resistance, flows through the voltage source and flows through the switch S_{A3} and flows through the switch S_{A2} and ends with the voltage source. In order to get negative half voltage, the switches S_{B2} , S_{B1} and S_{A3} will conduct. The current starts from voltage source V_{S2} and flows through the switch S_{A3} , S_{B1} and S_{B2} and ends with the voltage source V_{S2} . To get negative peak voltage, the switches S_{A1} , S_{B2} and S_{A3} will conduct. The current starts from the voltage source V_{S2} and flows through the switch S_{A3} , resistance, switch S_{A1} , voltage source V_{S1} , switch S_{B2} and ends with the voltage source V_{S2} .

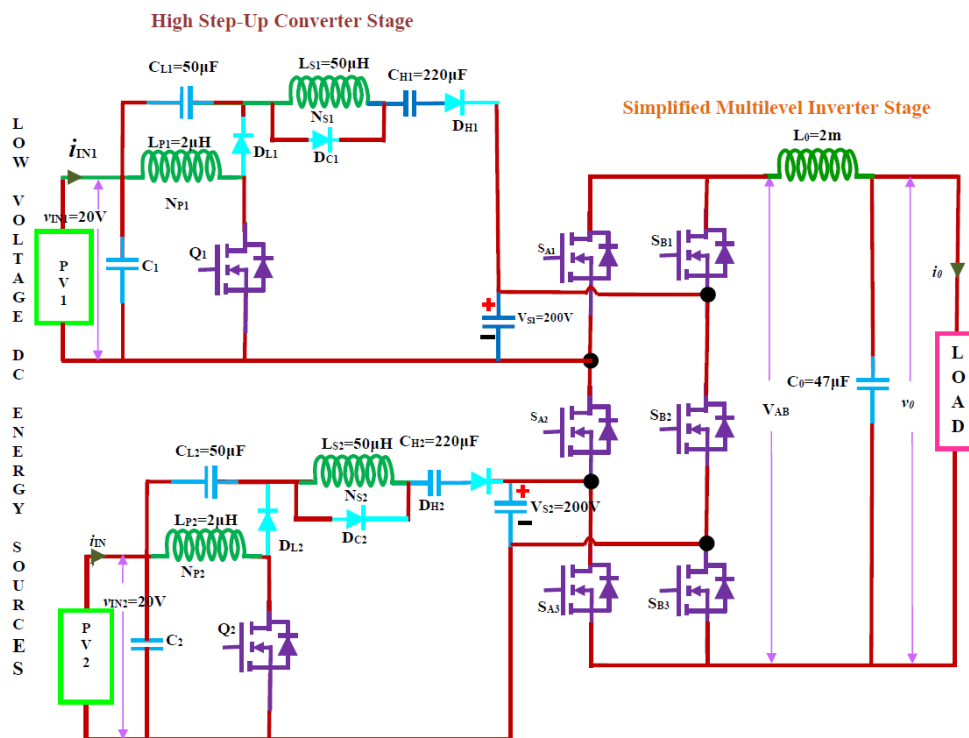


Fig 1. Single phase multi-string five-level inverter topology

3 DC-DC Converter

The dc-dc converter control flow is depicted in Figure 4. The voltage generated using the solar panel is given as input to the dc-dc converter. The dc ripple voltage in the capacitor has frequency twice the output frequency. If there is ripple voltage in the solar panel output, the function of maximum power tracking is affected. This has led to the inclusion of an inner current loop. This loop will help to produce constant reference current. This will remove the voltage variations to be developed in the link voltage. The solar panel output voltage and the primary inductor current are sensed using sensors. The MPPT controller receives the current and voltage values to calculate output voltage from the solar panel. The voltage from the panel and the voltage from the primary sensor are sent to the PI controller. This is used to generate the reference current for the current control loop. This current is sent to the amplifier to produce the trigger pulses for the converter switch S.

4 Maximum Power Point Tracking

The extraction of maximum power using the solar panel is a fixed voltage and current for all the conditions. But the maximum power extracted from the solar panel varies with climatic conditions. The current obtained from the solar panel varies with the irradiation level and the voltage across the panel varies with the temperature of the solar panel. It has to be ensured that maximum power is extracted from the panel even during variable load conditions. By controlling the current and voltage using a suitable dc-dc converter between the solar panel and the load, maximum power extraction from the panel can be obtained. It

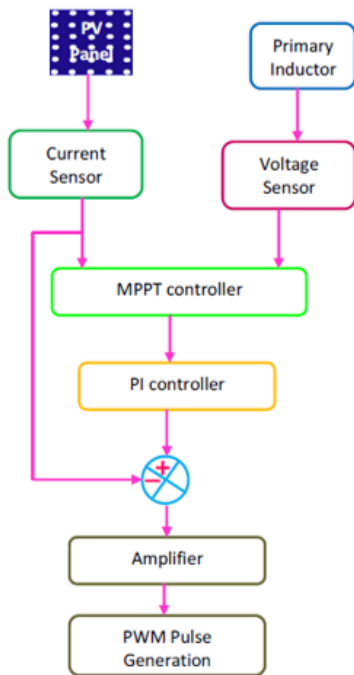


Fig 2. Flowchart for Triggering Pulse Generation

is possible to obtain maximum power transfer for all the operating conditions.

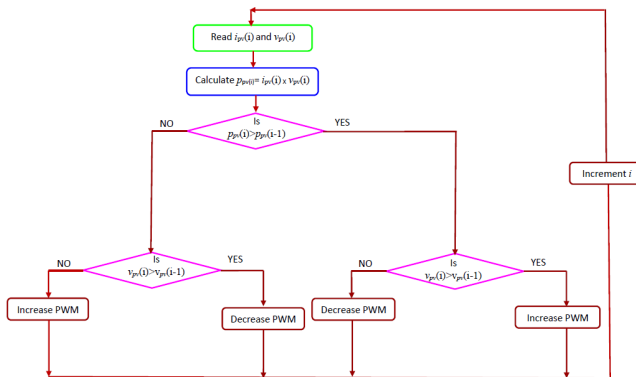


Fig 3. Flow chart for MPPT

In this paper, a dc-dc high step up converter with control algorithm between the solar panel and the inverter input terminals provides the maximum power transfer from the solar panel. There are many control algorithms developed for the extraction of maximum power from solar panel. This is done by measuring the initial voltage and current obtained from the solar panel. The purpose of the control algorithm in the converter circuit is to change the triggering angle so that maximum power is extracted from the solar panel with the available climatic conditions.

The logical sequence used for the maximum power tracking is shown in Figure 3. Generally, digital controllers like microcontrollers or DSP processors are used for the implementation of control algorithms. In order to supply power to ac loads, the low voltage signal from the solar panel is changed to high voltage.

5 Inverter Topology

In the case of conventional five level inverter circuits, there are bulky element connections and more complex control circuits. In order to simplify the five-level inverter structure, two capacitors are used and are connected across the dc bus.

Table 1. Switching Sequence of Inverter Switches

SWITCHES						VOLTAGE
S _{A1}	S _{A2}	S _{A3}	S _{B1}	S _{B2}	S _{B3}	V _{AB}
L	H	L	H	L	H	2V _s
L	H	H	H	L	L	V _s
H	H	L	L	L	H	V _s
H	H	H	L	L	L	0
L	L	L	H	H	H	0
H	L	L	L	H	H	-V _s
L	L	H	H	H	L	-V _s
H	L	H	L	H	L	-2V _s

The voltage level is controlled using the high step up converter. Thus, there are two voltage sources of 200V each. The CCHB inverter topology uses eight power switches for its operation. This topology uses phase shift pulse width modulation in the control circuit to generate pulses for the switches. When the switches S_{B1}, S_{A2} and S_{B3} are turned on to operate, the maximum voltage 2V_s appears across the output. Similarly in order to obtain maximum negative voltage in the output, the switches S_{A1}, S_{B2} and S_{A3} are made ON. The medium level voltage V_s is obtained by operating the switches S_{B1}, S_{A2} and S_{A3} or S_{A1}, S_{A2} and S_{B3}. Similarly, a negative value of medium level voltage is obtained by switching ON the switches S_{A1}, S_{B2} and S_{B3} or S_{B1}, S_{B2} and S_{A3}. The zero-voltage level can be obtained by short circuiting one of the arms of the inverter across the load terminals. In the conventional method, the switching loss caused in circuit is proportional to 8V_sf_s. All the switches are operating at switching frequency. The proposed method uses phase shift of pulse width modulation control scheme to develop the control signal. This topology uses six switches for its operation in which two switches are operating at low frequency, 50Hz. But the proposed converter has switching losses which are proportional to 4V_sf_s. The switching loss expression clearly states that the switching loss of the developed inverter is half that of the CCHB inverter.

6 Mathematical Analysis

The circuit analysis is done on the assumption that all the elements used in the circuit are ideal in characteristics. The current through the primary side of the inductor increases linearly as the switching device is changed to ON state. Since the conduction is discontinuous, the increase in current is from zero and can be expressed as (1)

If the time interval during which the increase in inductor current occurs is taken as DTs, then the change in the inductor current is given below

The on time of the device can be expressed in terms of D and T_s. T_s is the time period of one high-frequency switching cycle. At the end of increase of current, the maximum value is obtained and is given by (3)

The increase in the current waveform and the maximum value of current are shown in Figure 2. When the switch Q is turned off, the inductor current starts decreasing and reaches zero value. During this time interval, the primary inductor stores energy and is transferred to the capacitor. The discharging time comes to end, the current flowing through the primary inductor current becomes zero and the time interval to reach zero current is given by (4)

The primary inductor current is found out by integrating the current waveform over a cycle and is calculated as below.(5)

During the operation, the voltage across the primary inductor V_L is equal to the input voltage V_{PV}. Therefore, it can be written as (6)

The inductor voltage V_I can be expressed in terms of transformer turns ratio and V_L as below (7)

Now, the voltage V_B can be written as (8)

In order to have discontinuous conduction, using the voltage second balance equation, the inductor voltage V_L in the low voltage side to become zero is written as (9)

After simplification, the above equation becomes (10)

Since the voltage V_{CL} across capacitor C_L is equal to negative of the inductor voltage V_L in the low voltage side, voltage V_{CL} across capacitor C_L can be written as below (11)

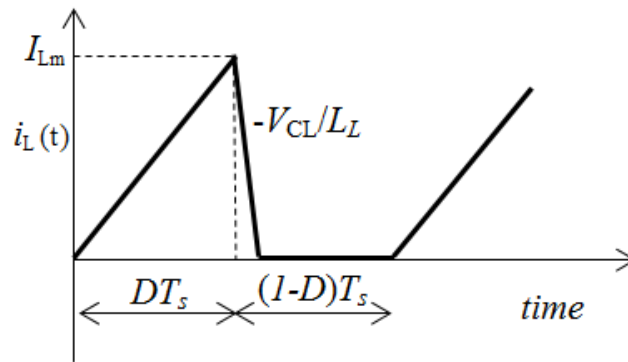


Fig 4. Waveform of $i_L(t)$

Using Kirchhoff’s voltage law, the voltage V_B of the converter can be written as (12)

The inductor voltage V_L in the secondary to become zero is written as

From equations (11) – (13), the voltage gain of the converter is written as

Voltage gain (14)

In the inverter operation, the voltage variation has to be limited in the specified value. This is done by designing the capacitor. The power relation for the design is based on the assumption that the difference between the power obtained from the PV source and the power delivered to the load is stored in the capacitor. The capacitor power is given by

$$P_C = P_{pv} - P_0$$

The net power difference is zero, the instantaneous power difference is stored in the capacitor. The difference voltage is taken as 10Volts. Based on this the capacitance calculated is around 2mF. The filter elements are calculated using the assumption that switching frequency is greater than $1/\sqrt{C_0L_0}$.

7 Results

It is important to know the performance of the proposed converter, comparative simulations and experiments with the conventional method are carried out. The values of the various components used in the circuit are shown in Table 2.

Table 2. Component Parameters of the proposed topology

High Step-up Converter Side Components		
Component	Symbol	Value
Input low voltage source	V_{IN1}, V_{IN2}	12V
Input high voltage source	V_{S1}, V_{S2}	200V
Switching frequency	f_s	50KHz
Primary Inductance	N_{P1}, N_{P2}	2 μ H
Secondary Inductance	N_{S1}, N_{S2}	50 μ H
Filter Capacitor in low voltage side	C_{L1}, C_{L2}	50 μ F/50V
Filter Capacitor in high voltage side	C_{H1}, C_{H2}	20 μ F/500V
Capacitor in clamped circuit	C_{C1}, C_{C2}	90 μ F/250V
Middle voltage Capacitor	C_{M1}, C_{M2}	10 μ F/500V
Bus Capacitor	C_{S1}, C_{S2}	2000 μ F/400V
Inverter side Components		
Output inductor	L_0	2mH
Output Capacitor	C_0	47 μ F/500V

Figure 5 shows the PV current obtained from the solar panel and Figure 6 shows the PV voltage of the solar panel. The diode current for the medium voltage is shown in Figure 7. The drain to source voltage of the inverter switches SA1 is shown in Figure 8. The output voltage is shown in Figure 9.

7.1 Simulation Results

The harmonic content of the output voltage V_{AB} can be calculated from the magnitude of the fundamental and harmonic components using MATLAB software for both the CCHB inverter and the proposed inverter. Both the CCHB inverter and the proposed inverter are made to operate at the similar conditions by selecting the switching frequency of operation is 50 kHz

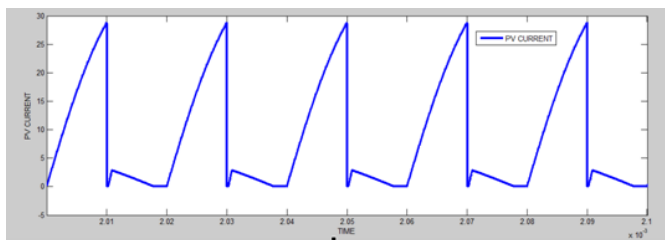


Fig 5. PV current waveform (Simulation)

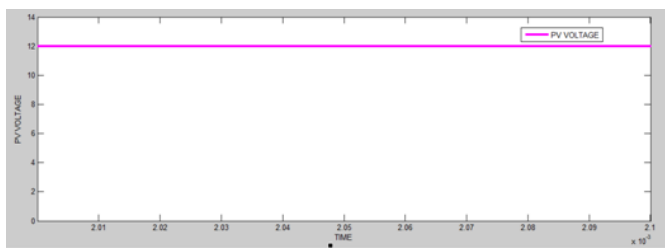


Fig 6. PV voltage waveform (Simulation)

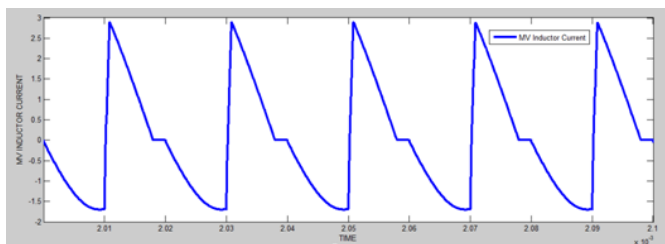


Fig 7. MV diode current (Simulation)

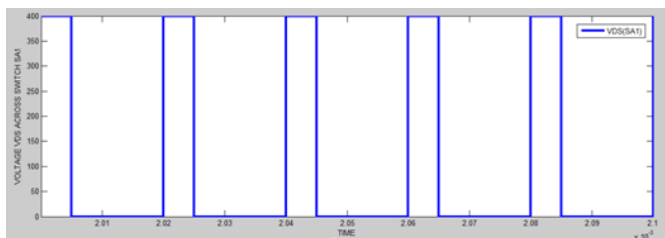


Fig 8. Voltage V_{DS} in S_{A1} (Simulation)

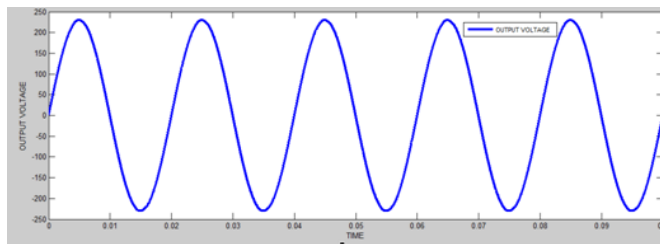


Fig 9. Output Voltage (Simulation)

Table 3. Harmonics of V_{AB} for CCHB five-level Inverter

Harmonic order	Amplitude(M=0.6)	Amplitude (M=0.7)
1	248.5V	267.8V
3	14.9V	13.6V
5	7.457V	6.1V
9	3.6V	2.3V
11	0.7V	0.6V
%THD of v_0	18.09	15.56

The modulation index values considered are $M=0.6$ and $M=0.7$. The low voltage side input voltage is $v_{IN1} = v_{IN2} = 20V$. The input voltage to the inverter is $V_{S1} = V_{S2} = 200V$. Table 3 and Table 4 show the simulation results of harmonic components and THD of the CCHB inverter and the proposed inverter respectively.

Table 4. Harmonics of V_{AB} for Proposed five-level Inverter

Harmonic order	Amplitude (M=0.6)	Amplitude (M=0.7)
1	268.9V	292.4V
3	8.3V	7.1V
5	6.9V	5.8V
9	1.5V	1.2V
11	0.24V	0.19V
%THD of v_0	2.99	2.84

It can be concluded from Table 3 and Table 4 that the THD level of the CCHB inverter and the proposed converter are compared; it shows that THD of CCHB is preferable. The proposed inverter voltage waveform is better than the CCHB inverter. The filter elements in the proposed converter are smaller in size than the CCHB topology.

7.2 Experimental Results

The inverter is designed for 200watts with an output voltage of 200 volts having the switching frequency of 50KHz and the operating line frequency of 50Hz. The experimental results of the developed microcontroller based five level inverter for the PV system are taken. The control of the pulse width is done using the PIC microcontroller of PIC16F877. The voltage developed across the switches is obtained from the test results. The switches are undergoing lower stress than the CCHB inverter.

The experimental results of the PV panel output are measured and it shows a steady value of voltage for the irradiation level as shown in fig.14. The diode current for the medium voltage and low voltage from the prototype are shown in fig. 15. The drain to source voltage of the inverter switches S_{A1} , S_{A2} are shown in fig. 16and fig.17. Fig. 18 shows steady state waveforms of output voltage v_0 and output current i_0 for the inverter with a resistive load of 40Ω . The conversion efficiency of the implemented inverter in this case is approximately 94%.

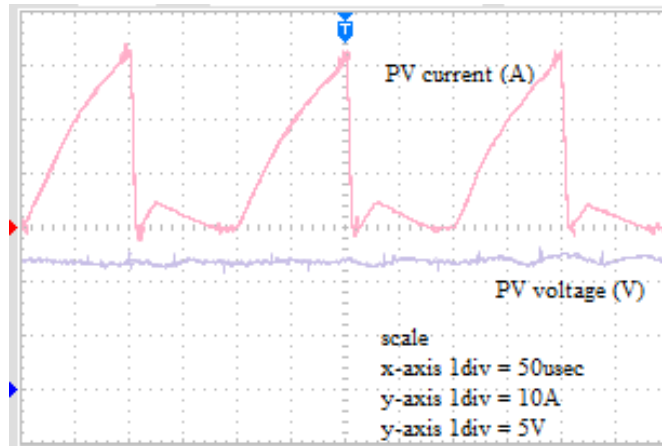


Fig 10. PV current and PVvoltage (Experimental)

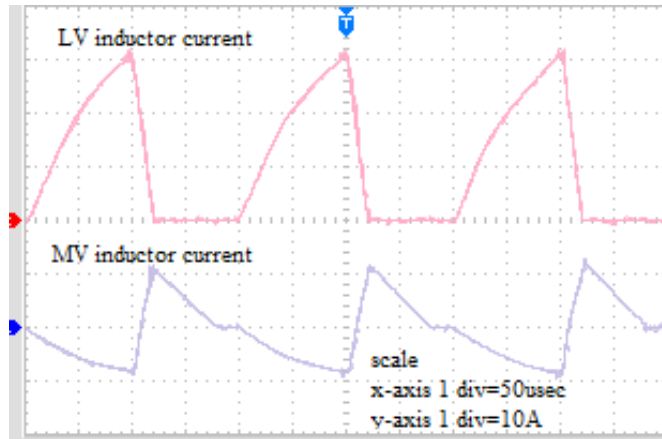


Fig 11. 10 diode current and LV diode current (Experimental)

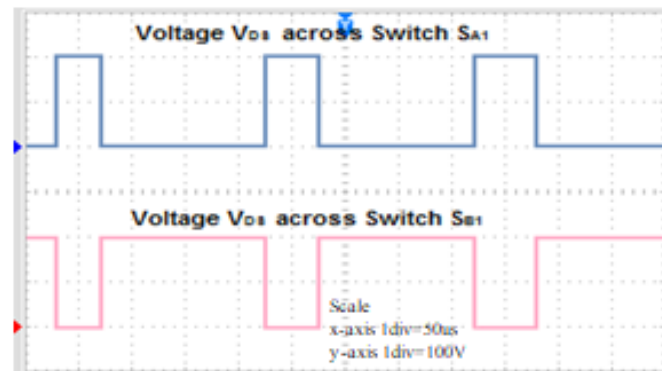


Fig 12. Voltage V_{DS} in S_{A1} & S_{B1} (Experimental)

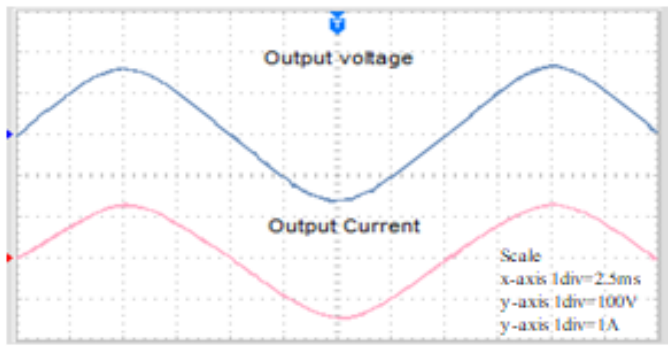


Fig 13. Output Voltage and Current (Experimental)

8 Discussion

The temperature of the surrounding environment is 36.2 and the solar radiation was 1000W/m². The solar panel temperature was 55. The power obtained from the solar panel was 200W. The output voltage from the solar panel is steady and stable. The implementation of the MPPT algorithm has produced a control signal based on the panel voltage and inductor current. Maximum power tracking is done effectively. The output current and voltage of the inverter after filtering the harmonics was sinusoidal waveform. From the %THD of the output voltage, it can be concluded that harmonic balance is obtained with the proposed system. The capacitors are performing the operation of energy balancing. The ripple voltage is controlled within the limits. The comparison of the proposed converter configuration with other types of inverter topology is given in Table 5.

Table 5. Comparison of different types of inverter components

Type/ Parameter	Diode Clamped ⁽¹⁴⁾	Flying Capacitor ⁽¹³⁾	Neutral Point clamped [22]	Cascade H-Bridge [30]	Proposed
Capacitor	4	4	3	2	2
Sources	1	1	1	2	6
Voltage Balancing	hard	hard	hard	hard	easy
High Frequency switches	8	8	6	8	6

The stress produced in the switches of the proposed converter is less. The performance parameters of some of the converters are discussed in Table 6. The five voltage levels are measured and the steady state performance of the proposed converter is analyzed. The voltage gain, efficiency and voltage stress of the proposed converter is compared with the other converters. The converter in papers ^{(1), (15)} can achieve high voltage gain at low values of duty cycle but the duty ratio is narrow. As compared to the converter in the paper ⁽³⁾, the proposed converter is able to get high voltage gain with reduced voltage stress. Also it can be noted that the current stress on the switches of the proposed converter is less as compared with the paper ^(16,17). The proposed converter is designed to provide required gain with a reduced voltage stress and current stress even for low duty cycle.

Table 6. Comparison of performance parameters

Paper	Voltage gain	Efficiency (%)	Maximum Voltage stress (V)
⁽¹⁾	2-6	93.7	665
⁽¹⁵⁾	16-38	97.0	40
⁽³⁾	3-5	96.6	256
⁽⁴⁾	30-90	96.6	100
⁽¹⁶⁾	4-8	92.5	24
⁽¹⁷⁾	10	95.9	60
proposed	12	94.0	200

9 Conclusion

The paper presents a new type of inverter developed for a PV system. The step-up voltage conversion of the generated dc voltage has been obtained using simple coupled inductor elements. The developed highly efficient high step up DC-DC converter is connected in the front end. This topology uses a single switch to attain the step-up operation. The proposed five-level inverter topology uses less number of switches required to implement multilevel output for PVs. The proposed inverter provides some advantages like better output waveforms with small size filter elements and lowers THD.

10 Limitations and future scope

The main drawback of the proposed configuration using coupled inductors is the leakage inductance, which may resonate with the parasitic capacitance of the switches. This may lead to high voltage peaks. Control circuit of the inverter is complex to find out the voltage level of the capacitors. These limitations are to be eliminated in the future work by implementing new techniques..

References

- 1) Jiawei Z, Daolian C, Jiahui J. Transformerless High Step-Up DC-DC Converter with Low Voltage Stress for Fuel Cells. *IEEE Access*. 2021;9:10228–10238. Available from: <https://doi.org/10.1109/ACCESS.2021.3050546>.
- 2) Lindiya SA, Palani S, Vijayarekha K. Modelling and Simulation of Photovoltaic System Fed Two Input Two Output DC-DC Boost Converter Interfaced with Asymmetric Cascaded H-Bridge Multilevel Inverter. *Indian Journal of Science and Technology*. 2017;10(5):1–9. Available from: <https://doi.org/10.17485/ijst/2017/v10i5/111139>.
- 3) Zhang X, Green TC. The Modular Multilevel Converter for High Step-Up Ratio DC-DC Conversion. *IEEE Transactions on Industrial Electronics*. 2015;62(8):4925–4936. Available from: <https://doi.org/10.1109/TIE.2015.2393846>.
- 4) Forouzesh M, Shen Y, Yari K, Siwakoti YP, Blaabjerg F. High-Efficiency High Step-Up DC-DC Converter With Dual Coupled Inductors for Grid-Connected Photovoltaic Systems. *IEEE Transactions on Power Electronics*. 2018;33(7):5967–5982. Available from: <https://doi.org/10.1109/TPEL.2017.2746750>.
- 5) Neti SS, Anand V, Singh V. Single-Phase Generalized Switched-Capacitor Multilevel Inverter Using Reduced Number of Power Semiconductor Components with Voltage Boosting Ability. *Arabian Journal for Science and Engineering*. 2022;47(3):2613–2627.
- 6) Yesuraj S, Ramadas G, Yesuraj J. High-power-factor single-switch AC to DC converter for LED lighting. *IEEE Transactions on Electrical and Electronic Engineering*. 2017;12(6):925–935. Available from: <https://doi.org/10.1002/tee.22484>.
- 7) Majumder MG, Rakesh R, Gopakumar K, Umanand L, Al-Haddad K, Jarzyna W. A Fault-Tolerant Five-Level Inverter Topology with Reduced Component Count for OEIM Drives. *IEEE Journal of Emerging and Selected Topics in Power Electronics*. 2021;9(1):961–969. Available from: <https://doi.org/10.1109/JESTPE.2020.2972056>.
- 8) Ramadas G, Nadesan MK, Yesuraj S, Yesuraj J. High power factor electronic ballast using resonant converter for compact fluorescent lamp. *International Journal of Circuit Theory and Applications*. 2017;45(1):95–109. Available from: <https://doi.org/10.1002/cta.2231>.
- 9) Muzamil HS, Mukhtiar AM, Abdul SL, Mohsin R. Design a Perturb & Observe MPPT Algorithm for PV System Based Asymmetric Cascaded Half-Bridge Multilevel Inverter. *Indian Journal of Science and Technology*. 2020;13(04):439–452. Available from: <https://doi.org/10.17485/ijst/2020/v13i04/149530>.
- 10) Alex T, Radhika S. Adaptive Voltage Control of High Step Up Converter for PV Applications. *Indian Journal of Science and Technology*. 2016;9(42):1–5. Available from: <https://doi.org/10.17485/ijst/2016/v9i42/104604>.
- 11) Siwakoti YP, Palanisamy A, Mahajan A, Liese S, Long T, Blaabjerg F. Analysis and Design of a Novel Six-Switch Five-Level Active Boost Neutral Point Clamped Inverter. *IEEE Transactions on Industrial Electronics*. 2020;67(12):10485–10496. Available from: <https://doi.org/10.1109/TIE.2019.2957712>.
- 12) Majumder MG, Yadav AK, Gopakumar K, R KR, Loganathan U, Franquelo LG. A 5-Level Inverter Scheme Using Single DC Link With Reduced Number of Floating Capacitors and Switches for Open-End IM Drives. *IEEE Transactions on Industrial Electronics*. 2020;67(2):960–968. Available from: <https://doi.org/10.1109/TIE.2019.2898594>.
- 13) Liao YH, Lai CM. Newly-Constructed Simplified Single-Phase Multistring Multilevel Inverter Topology for Distributed Energy Resources. *IEEE Transactions on Power Electronics*. 2011;26(9):2386–2392. Available from: <https://doi.org/10.1109/TPEL.2011.2157526>.
- 14) Yesuraj J, Parthiban S. LCC resonant converter with power factor correction for power supply units. *Journal of the Chinese Institute of Engineers*. 2015;38(7):843–854. Available from: <https://doi.org/10.1080/02533839.2015.1037995>.
- 15) Kumar P, Moursi C, Vinod MSE, Khalifa K, Tarek HAH, F HME. Novel Step-Up Transformerless Inverter Topology for 1- Φ Grid-Connected Photovoltaic System. *IEEE Transactions on Industry Applications*. 2021;57(3). Available from: <https://doi.org/10.1109/TIA.2021.3066141>.
- 16) Yang LS, Liang TJ, Chen JF. Transformerless DC-DC Converters With High Step-Up Voltage Gain. *IEEE Transactions on Industrial Electronics*. 2009;56(8):3144–3152. Available from: <https://doi.org/10.1109/TIE.2009.2022512>.
- 17) Chen LH, Fei L. Novel High Step-Up DC-DC Converter With an Active Coupled-Inductor Network for a Sustainable Energy System. *IEEE Transactions on Power Electronics*. 2015;30(12):6476–6482. Available from: <https://doi.org/10.1109/TPEL.2015.2429651>.